CHAPTER 319

MECHANISMS OF BEACH GROUND WATER AND SWASH INTERACTION

Andrew J. Baird[1], Travis E. Mason[2], and Diane P. Horn[3]

ABSTRACT

Previous studies of swash-ground water interactions have given prominance to infiltration of swash and backwash into unsaturated sand as the principal mechanism explaining sedimentation patterns in the inter-tidal zone. Here we consider the role of fluidisation in explaining such sedimentation patterns. It appears that fluidisation due to general ground water outflow from a beach is insufficient to induce fluidisation of surface sand. We propose a different mechanism for explaining fluidisation whereby very small amounts of swash infiltration into the seepage face cause rapid increases in pore water pressure below the beach surface. During the backwash, pressure unloading on the surface causes rapid ground water outflow from the surface sediment. The rate of this outflow is shown, using a simple model, to be sufficient to induce fluidisation. We also consider a model of general beach ground water behaviour and conclude that it can be satisfactorily used to provide boundary conditions for smaller scale models of fluidisation under swash.

1) INTRODUCTION

Grant (1946, 1948) was among the first to suggest a link between beach ground water behaviour and swash zone sediment transport. He proposed that a "dry" beach (one with a low water table, which he equated with unsaturated conditions below the beach surface) allows swash to infiltrate. The reduction in swash depth due to infiltration reduces swash velocity allowing sediment deposition. Therefore, a dry beach promotes accretion. Conversely, on a "wet" beach (one in which the water table is at or near the beach surface) the swash and backwash retain their depth because infiltration is limited. Backwash flows may be augmented by ground water outflow from the beach. Grant (1948) further suggested that the seepage force due to ground water outflow may

[1] Lecturer, Dept. of Geography, University of Sheffield, Sheffield S10 2TN, UK.
[2] Postgraduate research student, Dept. of Oceanography, Southampton Oceanography Centre, Southampton SO14 3ZH, UK.
[3] Lecturer, Dept. of Geography, Birkbeck College, University of London, London W1P 2LL, UK.

cause fluidisation of the sediment at the beach surface and enhance entrainment and sediment transport by backwash.

Infiltration

The logic of Grant's conceptual model has led many researchers to concentrate on the effects of infiltration losses on beach accretion and erosion (e.g. Emery and Foster, 1948; Emery and Gale, 1951; Isaacs and Bascom, 1949; Longuet-Higgins and Parkin, 1962; Duncan, 1964; Strahler, 1966; Harrison 1969,1972; Waddell, 1976; Chappell et al., 1979; Heathershaw, et al. 1981; Lanyon et al., 1982; Carter and Orford, 1993; and Turner 1993). Most of these authors have suggested that infiltration losses during swash provide the main mechanism by which beach accretion occurs above the still water level. However, despite the early suggestion of the importance of infiltration in the swash zone, few attempts have been made to model swash and backwash infiltration. Packwood (1983) developed a numerical model predicting runup due to a single bore incident on an initially dry beach. His justification for the development of this model was based on the assumption that infiltration is the mechanism that controls sediment transport on the beach face. Packwood (1983) argued that, as an incoming tide rises above the water table, the runup advances over dry sand and a proportion of the water mass is lost into the beach. Packwood's results showed that for fine sand (with a porosity, n, of 0.3, and a hydraulic conductivity, K, of 0.01 cm s^{-1}), very little water percolates into the beach. Packwood (1983) found that runup on fine sand and on an impermeable roughened slope are almost the same. In contrast, for medium sand (n = 0.3, K = 0.1 cm s^{-1}), although the maximum runup is reduced very little, the backwash is signficantly reduced in depth. This thin backwash layer drains rapidly into the sand, which will have a significant effect on the bed shear stress and the ability of the flow to transport sediment. Packwood (1983) concluded that the effect of a porous bed is seen much more in the backwash than in the swash. However, he did not consider the effect of a water table nearer to the beach surface on the infiltration process.

Fluidisation

In his 1948 paper Grant appears to suggest that the mechanism for fluidisation of sand grains on the beach surface is due to general ground water outflow from the beach associated with a high water table. A number of researchers have considered this effect but none have found convincing evidence of its importance in sand transport. For example, Oh and Dean (1994) used laboratory experiments and numerical modelling to investigate the influence of the beach water table on profile change and concluded that the effect of the upward flow on sediment transport appeared to be small compared with the effects of a steep slope. It seems likely that ground water outflow from a beach in response to a falling tide alone is insufficient to induce fluidisation, since hydraulic gradients under the beach surface will tend to be relatively small. It is proposed here that fluidisation is only generally possible in the presence of swash and that it occurs over relatively short timescales. As a swash flow advances over the saturated beach surface, there will be a relatively rapid increase in pore water pressures

below the beach surface. When under swash flow, the beach sediment behaves like a confined aquifer. The sediment is saturated and movement of water into the beach is extremely limited, since changes in porosity due to expansion and contraction of the mineral 'skeleton' will be minimal. However, because of this limited potential for infiltration, water pressures will propagate rapidly through the sediment. The characteristic time of propagation of any diffusion process is given by

$$t = \frac{x^2}{D} \qquad (1)$$

where x is distance (L) and D is the diffusivity ($L^2\ T^{-1}$), given by the ratio of hydraulic conductivity, K (LT^{-1}), to specific storage, s (L^{-1}). In a sand in the unconfined case, the specific storage multiplied by depth is called the specific yield and typically has values of between 0.1 and 0.3 per unit depth. In the confined case, which is effectively the case for sand under a swash lens, the specific storage is much lower and a value of the order of 0.002 is more realistic. The hydraulic conductivity of beach sands can be expected to be in the range 0.01 to 0.5 cm s^{-1} (Packwood and Peregrine, 1980). For all of the values in this range, the small value of specific storage will give relatively large values of D and small times of propagation, so that the pressure acting on the sand surface under advancing swash will propagate at least into the surface layers of the beach sediment. As the swash retreats there will be a release of pressure on the beach, giving large hydraulic gradients acting vertically upwards immediately below the surface. The resultant seepage force associated with rapid ground water outflow could be sufficient to induce fluidisation of the sand grains at the beach surface. This may occur during the latter stages of backwash and will provide readily entrainable material that can be carried seaward by the backwash flow. To our knowledge this mechanism has not been previously identified and no attempt has been made at modelling it. Later in this paper, we consider in detail how the propagation of pressure through the beach sediment can be modelled. However, whether infiltration into unsaturated or saturated sand is being considered, a first stage in any modelling exercise is the accurate prediction of the position of the seepage face together with predictions of more general ground water flows and pore water pressures within the beach, since these will act as boundary and initial conditions for infiltration and pressure propagation models. Below we consider how the general ground water behaviour of a beach can be modelled.

2) MODELLING BEACH GROUND WATER BEHAVIOUR

Theory

Recently, we have developed a model capable of predicting water table elevations in, and the extent of the seepage face on, sandy beaches. The model, called **GRIST** (**GR**ound water **I**nteraction with **S**wash and **T**ides), has been developed as a modular package and is described in Baird and Horn (1996) and Baird et al. (in review). Two approaches, both based on Darcy's Law and the continuity equation, have been used for modelling water table behaviour in response to tidal forcing in sandy beaches in the

GRIST package. The first approach uses the one-dimensional form of the Boussinesq equation given by

$$\frac{\partial h}{\partial t} = \frac{K}{s}\frac{\partial}{\partial x}\left(h\frac{\partial h}{\partial x}\right) \tag{2}$$

where h is the elevation of the water table (L), t is time (T), K is the hydraulic conductivity of the beach sediment (LT^{-1}), s is the specific yield or drainable porosity (dimensionless), and x is horizontal distance (L). The main assumption in using this equation is that ground water flow in a shallow aquifer can be described using the Dupuit-Forchheimer (D-F) approximation. D-F theory states that in a system of shallow gravity flow to a shallow sink when the flow is approximately horizontal, the lines of equal hydraulic head or potential are vertical, and the gradient of hydraulic head is given by the slope of the water table. Using D-F theory, two-dimensional flow to a sink can be approximated as one-dimensional flow, and the resulting differential equation (equation (2)) is more readily solved. In beaches which are underlain by relatively impermeable solid rock or clay deposits it is likely that D-F theory will provide adequate descriptions of ground water flow. The second approach used in the **GRIST** model considers the beach as a two-dimensional flow system in which the water table is a free surface or flow line. The advantage of the second approach is that it can be used to predict radial flow towards the seepage face if such an approach is necessary; for example, in cases where the flow field in the beach suddenly narrows forcing water to the surface.

Both equations have been solved in the **GRIST** package using standard finite-difference methods and are described in detail in Baird et al. (in review). In the 1D model, a block-centred finite-difference scheme is used and tide-water table decoupling is assumed to occur if

$$h_{i,t} + \left(\frac{(Q_i - Q_{i+1})\Delta t}{s_i}\right) > e_i \tag{3}$$

where Q_i is the rate of ground water discharge ($L^3\ T^{-1}$) (in a seaward direction) into cell i during Δt (from cell i-1), Q_{i+1} is the rate of discharge out of cell i during Δt, and e is the cell height (L). Further details of the model can be found in Baird and Horn (1996).

Field testing of the 1D model

The predictions of the 1D version of the model have been tested against field measurements which are described in detail in Baird et al. (in review). The field measurements were made on a microtidal beach at Canford Cliffs, Poole, Dorset, England. Canford Cliffs beach is a groyned beach and is backed by a sea wall. It has a mean slope of 3.2° (tan $\beta = 0.056$) on the upper foreshore and a mean slope of 1.5° (tan $\beta = 0.026$) on the lower foreshore. The tidal range at Canford Cliffs varies between 0.2 and 1.8 m on neap and spring tides respectively. The field measurements which are reported here were taken between the 21st and 28th October 1995 in a period leading from a neap to a spring tide, with a tidal range varying from 0.9 to 1.7

m. The significant wave height (H_s) varied from 0.35 to 0.76 m, while H_{rms} (root mean square wave height) varied between 0.25 and 0.53 m. Zero-crossing period varied between 5.2 and 6 s, and the peak spectral period varied between 5.6 and 9.8 s.

Water table elevations were measured with pressure transducers in ten screened wells placed at distances of 1.9, 3.8, 5.8, 7.8, 9.3, 10.8, 13.1, 15.6, 18.7, and 21.7 m seawards from the sea wall. Wave and tidal frequencies and amplitudes were measured with a seabed-mounted pressure transducer located at the low water mark. All instruments were logged using a PC at the top of the beach and were calibrated before and after the deployment. Beach profiles and instrument locations were measured using a total station. Sediment samples were collected at 0.5 m intervals along a cross-shore transect from the surface of the beach and at a depth of 20 cm for estimation of particle size parameters. Twelve sediment cores were also collected along the cross-shore transect for laboratory determinations of K using a constant head permeameter.

Results

The mean grain diameter of the surface sediments was approximately 0.24 mm (2.06 ϕ), the mean sorting was 0.44 ϕ and the mean skewness was -0.71. Results from 20 cm depth were very similar with a mean grain diameter of 0.22 mm (2.17 ϕ), a mean sorting of 0.36 ϕ and a mean skewness of -0.64. The mean K of the sediment cores was 0.225 cm s^{-1}, with a range from 0.036 to 1.179 cm s^{-1}, and a coefficient of variation of 143 per cent which is typical for this parameter.

The 1D model was run for Canford Cliffs using 40 computational cells with a width of 1 m. Measured values of tidal elevation were used in the simulation. The inland boundary was a no-flow condition at the sea wall. The bottom boundary was a no-flow condition given by the position of an impermeable barrier located 50 cm below Ordnance Datum. The seaward cell was assumed to be permanently saturated; that is, the water table was assumed to be always at the cell surface. A value of K/s of 0.75 cm s^{-1} was used in the model simulation. This value was calculated using the arithmetic mean of the permeameter measurements of K (0.225 cm s^{-1}) and an assumed value of s of 0.3.

The predictions of the 1D model are shown for each of the wells in Baird et al (in review). Here we show only two examples of the model's predictions, for wells 6 and 10 (9.3 and 1.9 m seaward of the seawall, respectively). In both cases the remarkably good agreement between modelled and observed water table elevations can be seen. The agreement was similarly good for all ten wells. Thus the model was able to predict with some accuracy water table rise and fall at different positions in the beach, giving a good representation of changes in the shore-normal water table profile over time. For most of the wells the model very accurately describes the lag and asymmetry of water table response. The predictions of lag and asymmetry are less good for wells 8 to 10, with the model predicting a later and steeper rise than was observed. The earlier rise of the observed water table may be due to setup and runup above the shoreline causing a greater flow of water into the beach than would occur due to tidal rise alone (see below). This point is discussed in more detail in Baird et al. (in review). It is also possible that the K of the sediment at the back of the beach was lower than that more seaward, giving greater lags than predicted by the model which uses a single value of

K. However, such a pattern of variation in K was not evident from the hydraulic conductivity data although it is recognised that surface sand samples may not be representative of sand at depth.

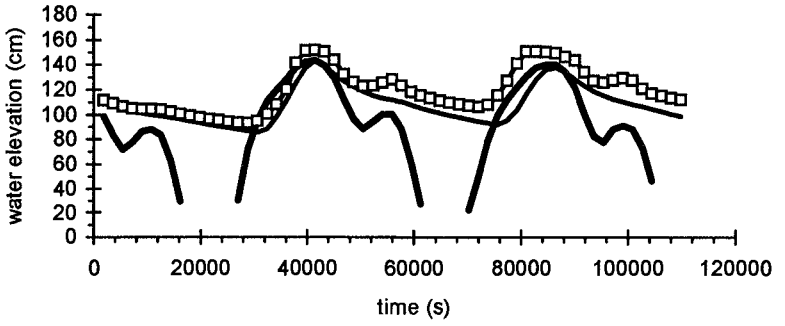

Figure 1. Measured and modelled water table elevations at well 6 (9.3 m seaward of sea wall). Open squares - observed; medium solid line - simulated; thick solid line - observed tide. Elevations given above a datum which represents the position of the impermeable barrier below the beach surface. Time is from 20.00 GMT on 22nd October 1995.

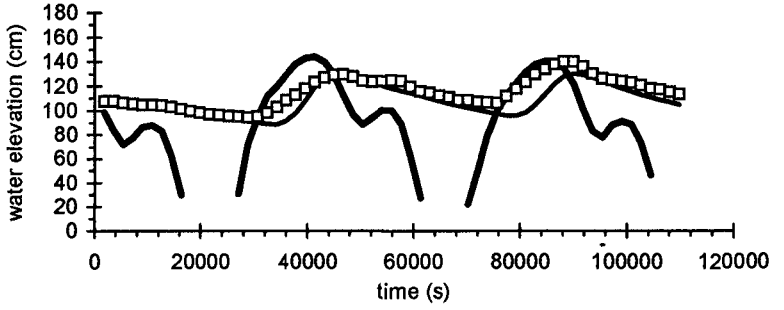

Figure 2. Measured and modelled water table elevations at well 10 (1.9 m seaward of sea wall). Open squares - observed; medium solid line - simulated; thick solid line - observed tide. Elevations given above a datum which represents the position of the impermeable barrier below the beach surface. Time is from 20.00 GMT on 22nd October 1995.

The agreement between observed and simulated water tables is better before high water at 40000 s than after. This is probably due to the fact that wave heights and swash excursions were greater after this time. The wave record shows that through the period of measurement H_S increased from 0.35 to 0.76 m. Setup and swash excursion

can be expected to give higher water tables than would be expected due to the tide alone and this is indeed the case with the observed water tables, with levels in well 6 in particular rising above high tide levels (Figure 1). A water table elevation above the high tide elevation is only possible if an additional source of water, such as rainfall, is entering the beach, or if setup and runup raise the mean water surface causing greater rates of flow into the beach. Greater setup due to the larger wave heights at high tide will increase the elevation of the shoreline. This, in turn, will give rise to greater amounts of seepage into the beach than would occur if the free surface on the beach face were at the tide level. Runup will increase water table levels via vertical infiltration and downward movement of water through the unsaturated zone. No rainfall was recorded during the measurement period reported here, so the source of additional water is most likely to be setup and runup. It is also possible that the increased departure between modelled and observed is due to accumulated error in model predictions since a small error in water table predictions will feed into later predictions. However, error propagation will tend to be cumulative whereas the figures clearly show that the discrepancy between observed and predicted occurs more as a step change during the second high water. Thus setup and runup are the more likely explanation for most of the discrepancy between observed and predicted.

The model based on equation (2) provides a good description of water table dynamics in response to tidal forcing although an allowance should be made in future versions of the model for the effects of setup. We suggest, therefore, that the model can be used to provide satisfactory boundary conditions for swash infiltration and pressure propagation models.

3) THE POSITION OF THE WATER TABLE RELATIVE TO THE BEACH SURFACE

Figure 3 shows the measured position of the water table relative to the sand surface for two positions of the tide, low water at 22800 s and high water at 40000 s. At low water the water table intersected the beach face at a distance of about 32 m from the sea wall (the tide was below the level of the beach shown on the diagram) and tended to approach the beach face at a tangent as suggested by Bear (1972). The water table in wells 1 and 2 fell little during the period between low water and subsequent immersion by the rising tide. Thus during the advance of the tide over the seepage face and later across the zone between 18 and 32 m from the sea wall, where the water table remained close to the beach surface, there would have been little opportunity for significant swash infiltration. Any infiltration that did occur is unlikely to have had an effect on swash and backwash dynamics during these conditions because the beach would have behaved like the impermeable case analysed by Packwood (1983). The water table at high water shows a pronounced landward slope and a superelevation of the water table in wells 6 and 7. This superelevation can be attributed to setup and runup as discussed above, and indicates that infiltration into this part of the beach may have the potential to affect swash and backwash hydraulics in the way described by Packwood (1983) for a permeable beach.

It would appear from the above reasoning that swash and backwash infiltration are only likely to be important in affecting swash/backwash hydraulics on a beach such as

Canford Cliffs during the latter part of the rising tide when some swash and backwash move over an unsaturated beach. However, it is important to stress that even small amounts of swash infiltration into the seepage face followed by rapid ground water outflow could induce fluidisation on middle and lower parts of the beach, and that the interaction between beach ground water behaviour and sediment dynamics may be more subtle than suggested by existing swash/backwash infiltration models such as that of Packwood (1983).

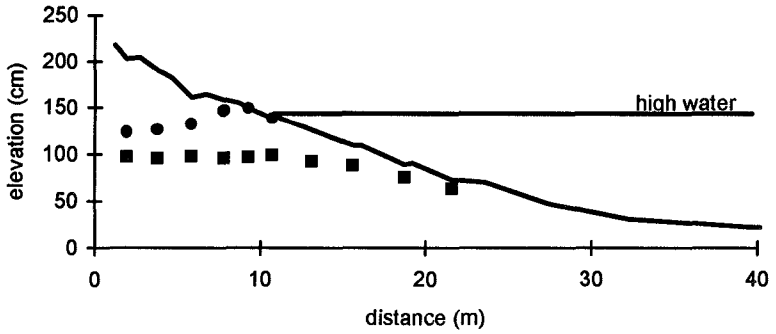

Figure 3. Measured water table elevations along the shore-normal profile at low water after an elapsed time of 22800 s (closed squares), and high water at 40000 s (closed circles).

4) MODELLING FLUIDISATION UNDER SWASH

It was noted earlier that when a swash runs over a saturated beach there will be a relatively rapid increase in pore pressure below the beach surface, and that the pressure release associated with backwash could induce fluidisation of the beach surface. The equation governing water movement through an isotropic and homogeneous saturated beach sediment is

$$\frac{\partial^2 h}{\partial x^2}+\frac{\partial^2 h}{\partial y^2}+\frac{\partial^2 h}{\partial z^2}=\frac{s}{K}\frac{\partial h}{\partial t} \qquad (4)$$

where here h is now the hydraulic head (L), and s is the specific storage (L^{-1}). For most purposes this equation can be simplified to its two-dimensional form.

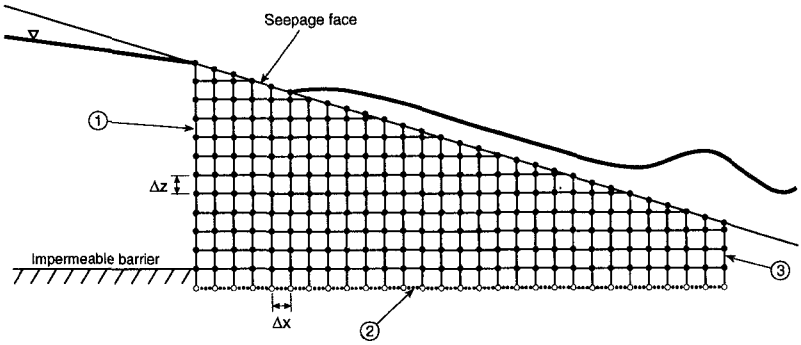

Figure 4. Finite difference grid for the simulation of pressure propagation into a sand bed under swash. ① and ③ are boundaries where the head is given. ② is a no-flow boundary.

The requirements of a two-dimensional model of ground water flow, and therefore pressure propagation, through beach sediment under advancing swash and retreating backwash are shown in Figure 4. The diagram shows a finite-difference, mesh-centred grid representing the body of sand beneath and landward of swash. For the upper boundary condition the model requires a time series of swash depths for that part of the beach face which becomes inundated. It is assumed that the pressure acting on the beach surface at the base of the swash is equivalent to the swash depth; that is, the pressure is hydrostatic. It is this hydrostatic pressure that provides an upper boundary condition to the model. The lower part of the model is assumed to be a no-flow boundary (von Neuman condition) which can be simulated using a set of fictitious nodes shown by open circles. The boundary condition $\partial h/\partial z = 0$ translates in finite-difference form to $h_{i,\,j-1} = h_{i,\,j+1}$ assuming an indexing notation whereby j represents row number (z axis - positive upwards) and i column number (x axis - positive to the right of the diagram). The impermeable barrier is given by j so that j-1 represents the fictitious nodes. The inland boundary condition is a prescribed head condition (Dirichlet condition) which can be provided either from field measurements or, as noted above, from a larger scale beach ground water model such as **GRIST**. In Figure 4 it is shown as the column of nodes below the exit point. The position of the exit point can also be provided from measurements or modelling. The seaward boundary condition is given by prescribed heads at the nodes. This distribution of heads can be assumed to be hydrostatic and equal to wave height at this point. The initial condition for the internal nodes can be estimated from field measurements or can be assumed to be a hydrostatic distribution of hydraulic heads.

Figure 4 represents an ideal solution to the problem of fluidisation under swash and backwash. In the absence of detailed information on the two-dimensional structure of swash, which we are currently measuring using capacitance probes and video techniques, we consider below the effect of water loading and unloading on a one-dimensional column of saturated sand. A simple explicit finite-difference method was used to solve the one-dimensional form of equation (4). The solution is given by

$$\frac{h_{j+1}^n - 2h_j^n + h_{j-1}^n}{(\Delta z)^2} = \frac{s}{K}\left(\frac{h_j^{n+1} - h_j^n}{\Delta t}\right) \quad (5)$$

where the superscript n refers to time.

Five cases of inundation were considered in the model simulations. In all model runs the initial distribution of hydraulic heads below the surface was assumed to be hydrostatic. Nodes were spaced 2 cm apart and the total column length was 60 cm. The base of the column was a no-flow boundary. The cases were:

Case 1. Step increase in pressure on the upper boundary equivalent to a water depth of 10 cm followed by a step return to a condition of no excess pressure on the surface. The pressure loading lasts for 3 seconds and the simulation lasts for 6 s. $K = 0.1$ cm s^{-1}; $s = 0.002$ cm^{-1}.

Case 2. As for Case 1 except that $s = 0.004$ cm^{-1}.

Case 3. Step increase in pressure on the upper boundary equivalent to a water depth of 5 cm followed by a step return to a condition of no excess pressure. The pressure loading lasts for 3 seconds and the simulation lasts for 6 s. $K = 0.025$ cm s^{-1}; $s = 0.002$ cm^{-1}.

Case 4. For a more realistic loading and unloading of water on the upper boundary we used Hughes' (1992) measurements of swash on beaches in Sydney, Australia (case 'a' from Figure 7a of Hughes, 1992). The actual swash depths were approximated using a ramp addition lasting for 2 s and a ramp loss of water lasting for 6.5 s, with a maximum water depth of 20 cm and a total period of inundation of 8.5 s. $K = 0.05$ cm s^{-1}, $s = 0.002$ cm^{-1}.

Case 5. As for Case 4 but with K=0.02 cm s^{-1}.

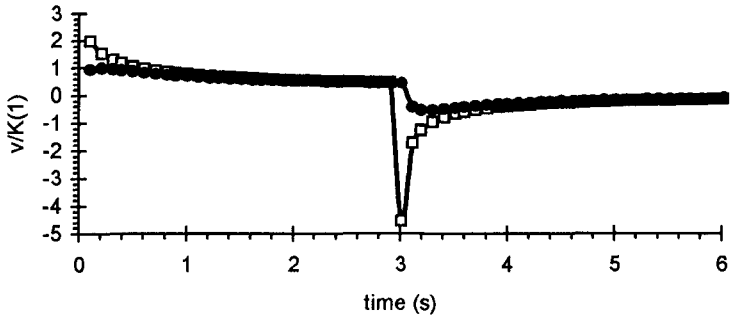

Figure 5. Variations in v/K over time for Case 1 (see text for details).

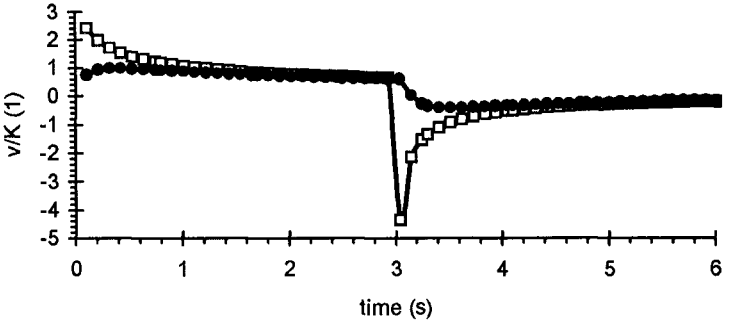

Figure 6. Variations in *v/K* over time for Case 2 (see text for details).

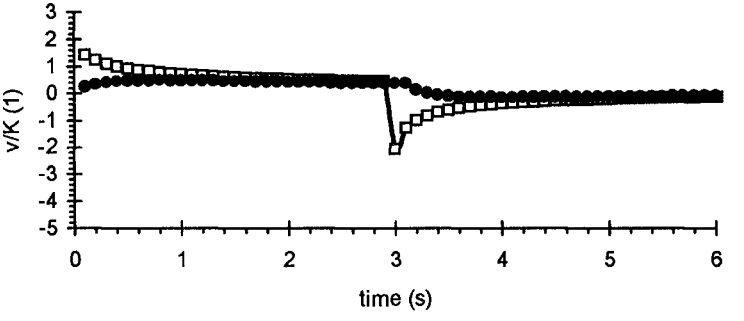

Figure 7. Variations in *v/K* over time for Case 3 (see text for details).

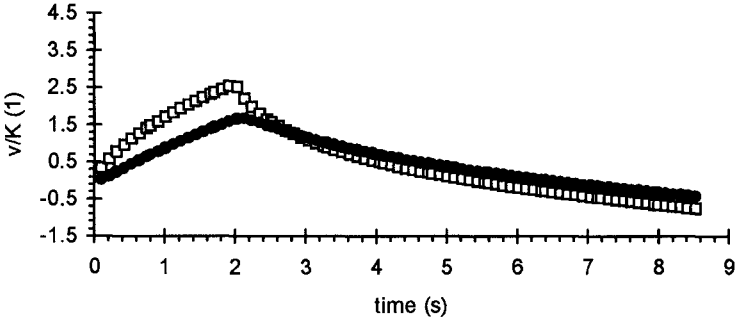

Figure 8. Variations in *v/K* over time for Case 4 (see text for details). Note the change in axes scales.

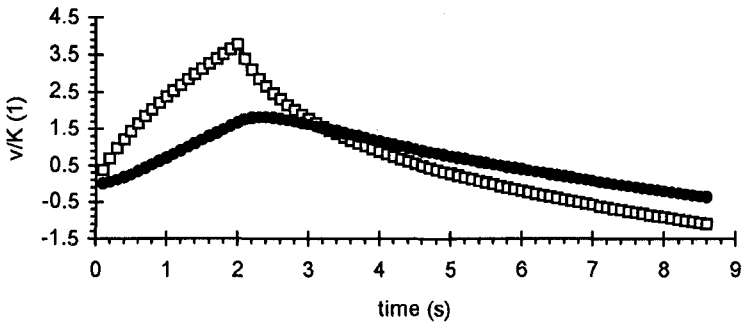

Figure 9. Variations in v/K over time for Case 5 (see text for details).

Cases 1 to 5 are illustrated in Figures 5 to 9, respectively. In each figure, v/K is plotted against time, where v is the specific discharge (cm s^{-1}) through the sand. v/K is equivalent to the hydraulic gradient. Two time series are shown. That with the open squares represents the hydraulic gradient acting between the node 2 cm below the surface and the node representing the beach surface. The closed circles represent the hydraulic gradient between the nodes 4 and 2 cm below the surface. A positive gradient indicates flow downwards into the sand, a negative gradient upward flow. The values of K and s used in Cases 1 to 5 are all within the range of what might be expected for fine to medium sand (see Packwood and Peregrine 1980).

Packwood and Peregrine (1980) noted that for most sands and fine gravels, fluidisation occurs when $v/K < -0.7$ (using the sign convention above). (See also Bear, 1972, pp. 184-189). Fluidisation occurs when the effective stress becomes zero. It should also be noted that downward seepage has the effect of increasing the effective stress and increasing the stability of the sediment. Cases 1 to 3 show that there is an initially large hydraulic gradient associated with the addition of water to the sand surface which declines in an approximately exponential fashion with time. After the removal of the ponded water there is a sudden reversal in the direction of the hydraulic gradient. In all three cases fluidisation can be expected to occur since v/K is less than -0.7. The period of potential fluidisation lasts for approximately 0.4 to 0.6 s. It is interesting to note that large values of v/K are only present in the uppermost layer of sand.

Under real swash, step loading and unloading is unlikely to occur, with the addition and removal of water being more gradual. As noted above, we used the measurements made by Hughes (1992) as a first approximation to loading and unloading under real swash. In Case 4 fluidisation is not predicted by the model. However, a reduction in the ratio of K/s, as shown in Figure 9 (Case 5), does give predicted fluidisation for approximately the last second of the backwash. Much more information is needed on swash and backwash velocities and shear stresses on the bed to understand the implications of this for sediment movement in the swash zone. However, the simple model is revealing in that it suggests that fluidisation of the bed occurs before the beach surface is exposed so that the entrainment and seaward transport of sediment in the

latter stages of backwash is enhanced. This is consistent with qualitative observations of backwash by Hughes (1992) who, with other workers, notes that as the swash lens thins during backwash it develops into a slurry of fluid and sediment. The one-dimensional model is obviously an over-simplification of pressure propagation through a sand bed under swash, as is the assumption of a single swash passing over the bed in which the initial condition is a hydrostatic distribution of hydraulic head. However, the model does suggest a mechanism for fluidisation in the swash zone apparently not previously considered by other workers, and one that may exert a greater control on sediment movement in the swash zone than infiltration of swash into the unsaturated part of the beach. It is important to stress that, although the mechanism described here involves infiltration into the sand bed, the amount of water lost from swash and backwash is negligible since the specific storage of saturated sand is so low. Thus it appears that infiltration *sensu* Grant (that is, infiltration into unsaturated sand above the water table) is not needed for ground water to have a significant impact on swash sediment dynamics. The mechanism of fluidisation given here is certainly worthy of further investigation, and to elucidate the processes involved we are engaged in measurements of swash/backwash flows and pressure propagation in both the laboratory and the field site at Canford Cliffs. Results from these studies will be reported in due course.

ACKNOWLEDGEMENTS

Most of the funding for this research came from the United Kingdom Natural Environment Research Council (Grant number GR9/01726). The remainder of the funding was from grants from Birkbeck College, University of London, and the University of Sheffield awarded to Horn and Baird respectively. We would like to thank Mike Wilkin, Paul Bentley, Peter Riley, John Cross, Steve Pearce, Matthew Foote, Simon Gaffney, Richard Kelly, Mark Lee, Chris Turner, Jill Ulmanis, and Steve Wallbridge for their help and advice. Finally, we would like to thank Poole Borough Council who kindly allowed us to use the Surf Lifesaving Club building at Canford Cliffs for housing logging equipment.

REFERENCES

Baird, A.J. and Horn, D.P. 1996. Monitoring and modelling ground water behaviour in sandy beaches. Journal of Coastal Research 12(3): 630-640.

Baird, A.J., Horn, D.P. and Mason, T.E. (in review). Validation of a beach ground water model. Submitted to Marine Geology.

Bear, J. 1972. Dynamics of Fluids in Porous Media, Elsevier, New York, 764 pp.

Carter, R.W.G. and Orford, J.D. 1993. The morphodynamics of coarse clastic beaches and barriers: a short- and long-term perspective. Journal of Coastal Research 15: 158-179.

Chappell, J., Eliot, I.G., Bradshaw, M.P. and Lonsdale, E. 1979. Experimental control of beach face dynamics by water-table pumping. Engineering Geology 14: 29-41.

Duncan, J.R. 1964. The effects of water table and tidal cycle on swash-backwash sediment distribution and beach profile development. Marine Geology 2: 186-197.

Emery, K.O. and Foster, J.F. 1948. Water tables in marine beaches. Journal of Marine Research 7: 644-654.
Emery, K.O. and Gale, J.F. 1951. Swash and swash mark. Transactions of the American Geophysical Union 32(1): 31-36.
Grant, U.S. 1946. Effects of ground water table on beach erosion. Bulletin of the Geological Society of America 57: 1252 (abstract).
Grant, U.S. 1948. Influence of the water table on beach aggradation and degradation. Journal of Marine Research 7: 655-660.
Harrison, W. 1969. Empirical equations for foreshore changes over a tidal cycle. Marine Geology 7, 529-551.
Harrison, W. 1972. Changes in foreshore sand volume on a tidal beach: role of fluctuations in water table and ocean still-water level. Proceedings of the 24th International Geological Conference, Montreal: 159-166.
Heathershaw, A.D., Carr, A.P., Blackley, M.W.L. and Wooldridge, C.F. 1981. Tidal variations in the compaction of beach sediments. Marine Geology 41: 223-238.
Hughes, M.G. 1992. Application of a non-linear shallow water theory to swash following bore collapse on a sandy beach. Journal of Coastal Research 8: 562-578.
Isaaks, J.D. and Bascom, W.N. 1949. Water table elevations in some Pacific coast beaches. Transactions of the American Geophysical Union 30: 293-294.
Lanyon, J.A., Eliot, I.G., and Clarke, D.J. 1982. Observations of shelf waves and bay seiches from tidal and beach ground water-level records. Marine Geology 49, 23-42.
Longuet-Higgins, M.S. and Parkin, D.W. 1962. Sea waves and beach cusps. Geographical Journal 128: 194-201.
Oh, T-M. and Dean, R.G. 1994. Effects of controlled water table on beach profile dynamics. Proceedings of the 24th International Conference on Coastal Engineering: 2449-2460.
Packwood, A.R. 1983. The influence of beach porosity on wave uprush and backwash. Coastal Engineering 7: 29-40.
Packwood, A.R., and Peregrine, D.H. 1980. The propagation of solitary waves and bores over a porous bed. Coastal Engineering 3: 221-242.
Strahler, A.N. 1966. Tidal cycle of changes in an equilibrium beach, Sandy Hook, New Jersey. Journal of Geology 74: 247-268.
Turner, I.L. 1993. The total water content of sandy beaches. Journal of Coastal Research Special Issue 15: 11-26.
Waddell, E. 1976. Swash-ground water-beach profile interactions. In Davis, R.A. and Etherington, R.L. (eds) Beach and nearshore sedimentation. Society of Economic and Paleontological Mineralogists Special Publication 24: 115-125.